perfluoroalkanesulfonic acids and derivatives that would be difficult to obtain by other methods. For instance, it should be straightforward to prepare perfluoroneopentanesulfonyl fluoride and perfluoro-2-butanesulfonyl fluoride from the hydrocarbon starting materials with elemental fluorine. In addition, perfluorotetramethylene sulfone was obtained along with one useful byproduct, perfluorobutanesulfonyl fluoride. The previously reported preparation of this perfluorinated cyclic sulfone involves at least six steps starting from tetrafluoroethylene, iodine, and elemental sulfur.[15]

Although the first successful fluorination of ethyl acetate has been accomplished in our research program,[14b] the instability of the ester linkage toward hydrogen fluoride produced by the fluorination makes fluorination of hydrocarbon esters still challenging. In fact, fluorination of esters by other methods produces only the corresponding perfluoroalkanoyl fluoride.[21] By contrast, fluorination of cyclic alkanesulfonic ester would be more challenging. In addition to the relatively weak carbon–sulfur bond, the sulfur–oxygen, oxygen–carbon, and even carbon–carbon bonds could be ruptured either by elemental fluorine or hydrogen fluoride. Our successful production of perfluoro-1,4-butanesultone is significant. The conventional preparation of a perfluorinated sultone, by reaction of tetrafluoroethylene with sulfur trioxide, allows only an even number of carbons in the cyclic system. Furthermore, no branched structural sultone can be obtained by this conventional method. The direct fluorination of corresponding hydrocarbon analogues opens the possibility of preparation of structurally different pendant groups on the perfluorinated polymers, which should be useful in the areas of electrochemical membranes, battery separators, and chromatographic separations.[11,22]

Acknowledgment. We are grateful for the support of this work by the Air Force Office of Scientific Research (Grant AFOSR-88-0084) and by a NATO grant to R.J.L. and H.R.

(21) Banks, R. E. *Preparation, Properties and Industrial Applications of Organofluorine Compounds*; John Wiley: New York, 1982; pp 19–43.

(22) Yeager, H. L.; Steck, A. *Anal. Chem.* **1979**, *51*, 862.

Contribution from the Chemistry Division and Intense Pulsed Neutron Source Division, Argonne National Laboratory, 9700 South Cass Avenue, Argonne, Illinois 60439

Hydrothermal Crystallization of Porphyrin-Containing Layer Silicates

K. A. Carrado,*,† P. Thiyagarajan,‡ R. E. Winans,† and R. E. Botto†

Received June 22, 1990

Porphyrins and metalloporphyrins have been demonstrated as organic templates in the hydrothermal crystallization of layered silicate smectite clays. Two water-soluble free-base porphyrins, tetrakis(*N*-methyl-4-pyridiniumyl)porphyrin (TMPyP) and tetrakis(*N*,*N*,*N*-trimethyl-4-aniliniumyl)porphyrin (TAP), along with metallo derivatives like Fe^{III}TAP, were utilized as their chloride salts. Aqueous gels consisting of a 0.0166:0.20:1.00:1.52 porphyrin:LiF:$Mg(OH)_2$:SiO_2 molar ratio heated at reflux temperature crystallized synthetic porphyrin-containing hectorite clays in just 2 days. X-ray powder diffraction (XRD) gave (001) reflections of 15.0, 16.7, and 16.4 Å for TMPyP–, TAP–, and FeTAP–hectorite, respectively, indicating that the organic macrocycles are intercalated parallel between the clay layers. Microanalysis data and UV–visible diffuse reflectance (DR) absorption spectra reveal that the porphyrin is incorporated intact. XRD and DR spectra also reveal that the free-base forms of the porphyrins dominate in hydrothermal crystallization products, while in ion-exchanged products the dication forms predominate. Small-angle neutron scattering (SANS) was used to follow the crystallization of these systems and to analyze interactions that exist when porphyrin is reacted with silica sol and magnesium hydroxide alone. Guinier analysis of the scattering curves yields structural information about the growth process of the clay system. Random network structures are observed for the porphyrin–silica system.

Introduction

Smectite clay minerals constitute a naturally occurring class of inorganic catalysts and supports. These minerals have layered lattice structures in which clay sheets are separated by layers of hydrated cations. Two tetrahedral silica sheets sandwiching a central sheet of octahedral sites form a 2:1 smectite clay layer.[1] The octahedral sites are occupied by aluminum in montmorillonite and by magnesium in hectorite. Substitution of Li^+ ions for Mg^{2+} ions in the octahedral sheet of hectorite causes a net negative layer charge, distributed over all oxygens in the framework, which is compensated by the interlayer cations. Ion exchange of these cations allows the introduction of organic and metal complex cations for a variety of applications.[2,3] The (001) reflection along the *c* axis is a measure of the distance between clay layers; this *d* spacing is a function of both the type of cation and the amount of water present.

Organic molecules are commonly used as templates in zeolite syntheses. Although their role as structure directors is under some debate,[4] small organic cations do exist in the pores and channels of the resulting zeolite crystallites. The influence of templates is both steric and electronic in these systems, and they typically exhibit the stoichiometry and space-filling characteristics illustrated for molecular sieves such as $AlPO_4$-5.[5] Assuming that silicate structures can be determined, at least in part, by the geometry of an encapsulated molecule, then the use of a large, flat macrocycle like a porphyrin should help to induce silicate layer formation. Among the few reports of synthetic clays made with organic molecules in the synthesis gel is one by Barrer and Dicks,[6] who prepared synthetic alkylammonium hectorites and montmorillonites. Porphyrin-containing hectorite clays have now been prepared from synthesis gels by using similar techniques, with a resulting reduction in reaction time from 5 to 2 days. The specific porphyrins used are the water-soluble chloride salts of tetrakis(*N*-methyl-4-pyridiniumyl)porphyrin (TMPyP) and tetrakis(*N*,*N*,*N*-trimethyl-4-aniliniumyl)porphyrin (TAP) and their metallo derivatives.

* To whom all correspondence should be addressed.
† Chemistry Division.
‡ IPNS Division.

(1) Grim, R. E. *Clay Mineralogy*; McGraw-Hill: New York, 1953.
(2) Pinnavaia, T. J. *Science* **1983**, *220*, 365.
(3) Carrado, K. A.; Winans, R. E. *Chem. Mater.* **1990**, *2*, 328.
(4) Lok, B. M.; Cannan, T. R.; Messina, C. A. *Zeolites* **1983**, *3*, 282.
(5) Flanigen, E. M.; Lok, B. M.; Patton, L.; Wilson, S. T. *Pure Appl. Chem.* **1986**, *58*, 1351.
(6) Barrer, R. M.; Dicks, L. W. R. *J. Chem. Soc. A* **1967**, 1523.

0020-1669/91/1330-0794$02.50/0

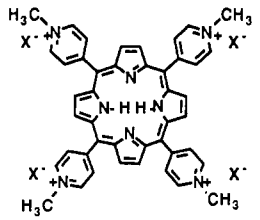

TMPyP

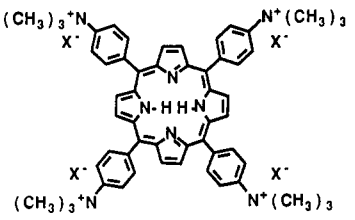

TAP

Experimental Section

Materials. The precursor gels were of composition

$$0.32\ R,\ 1.0\ LiF,\ 5.3\ Mg(OH)_2,\ 8\ SiO_2,\ n\ H_2O$$

to correlate with the ideal hectorite[1] composition

$$Ex_{0.66}[Li_{0.66}Mg_{5.34}Si_8O_{20}(OH)_4]$$

where R = organic base or salt and Ex = exchangeable monocation.

Syntheses were not successful when the cited[6] amount of R = LiF (0.66 mol) was used, whether the gel was allowed to react for 2, 5, or even 7 days. Aqueous gels consisting of a 0.06:0.20:1.00:1.52 organic:LiF:$Mg(OH)_2$:SiO_2 molar ratio worked best. A typical (scaled-down) reaction began by dissolving 0.72 mmol of organic (e.g. tetramethylammonium hydroxide or (TMA)OH) in water in a 250-mL round-bottom flask, to which 0.12 g (0.0048 mol) of LiF was added with vigorous stirring. Separately, 6.5 g (0.024 mol) of $MgCl_2{\cdot}6H_2O$ was dissolved in H_2O, and the mixture was allowed to react with 32 mL of 2 N NH_4OH to crystallize $Mg(OH)_2$, which was then centrifuged and washed with at least 4 volumes of water to remove excess ions. This was transferred with water to the organic–LiF slurry. After the slurry was stirred for 10–15 min, 9.73 g (0.036 mol) of Ludox HS-30, a Na^+-stabilized 30% silica sol (Du Pont), was slowly added and the total volume brought to about 150 mL (2–5 wt % solids were customarily used). After 2–3 days at reflux, crystallization was complete, as determined by the lack of $Mg(OH)_2$ reflections in X-ray powder diffraction spectra; these occur at 4.77 and 2.37 Å for the (001) and (101) reflections, respectively. Solids were centrifuged, washed, and air-dried. Syntheses for SANS experiments were cited out in D_2O rather than H_2O.

Since each porphyrin contains four positively charged groups, only 0.2 mmol of porphyrin was needed in the preparation outlined above. Thermal gravimetric analysis revealed that the porphyrins contain an appreciable amount of water (e.g.: (TMPyP)Cl, $C_{44}H_{38}N_8Cl_4{\cdot}6H_2O$, MW = 928; TAPCl, $C_{56}H_{62}N_8Cl_4{\cdot}11H_2O$, MW = 1186). The synthetic hectorites that incorporate organics into the synthesis gels are hereafter denoted as, for example, TMA–hectorite and TMPyP–hectorite. For comparison purposes in terms of characterization, simple ion exchanges of the porphyrins into previously made synthetic clays were also carried out. The purely inorganic synthetic hectorite, made by following the Barrer preparation,[6] has Li^+ exchangeable cations and is referred to as SLH (synthetic Li^+–hectorite). Ion exchanges were performed with 0.1 M solutions of (TMA)OH or 1×10^{-3} M solutions of porphyrin chloride salts stirred in contact with SLH for 18–24 hr and then centrifuged, washed, and air-dried. These clays are denoted as, for example, TMA–SLH and TMPyP–SLH.

All chemicals used were of reagent grade. Porphyrins were purchased from Midcentury Chemicals, Posen, IL. All water used was both distilled and deionized. A natural water-washed hectorite sample was used for control experiments in SANS. This material, called hectabrite AW (HAW), was used as received from the American Colloid Co. The supplier specifications for HAW are >85% hectorite with dolomite and calcite impurities (no quartz or cristobalite) with a clay composition of $(Al_{0.01}Li_{30}Mg_{2.67})Si_4O_{10}(OH)_2(Na,Ca)_{30}$.

Characterization. X-ray powder diffraction (XRD) was done on a Scintag PAD-V instrument using Cu Kα radiation and a hyperpure germanium solid-state detector; scan rates varied from 0.25 to 0.75° 2θ/min. The instrument was calibrated to the (101) reflection of low-quartz[7] at 3.34 Å. Oriented films were made by air-drying clay slurries on glass slides; powders were loosely packed in horizontally held trays. Data were collected on a DG desktop computer system.

UV–visible spectroscopy of solutions was performed on a Shimadzu UV-160 instrument in the slow analysis mode. Diffuse reflectance (DR) absorption spectra were recorded on a Cary 2390 spectrometer equipped with an integrating sphere accessory. All DR spectra were scanned at 1 nm/s; appropriate reference samples were run as automatic baselines prior to sample runs. The same slides used for XRD analysis were mounted vertically over the open port (about 1-cm diameter). Thermal gravimetric analysis (TGA) was done by using a Cahn 121 microbalance, interfaced to an IBM PC, under nitrogen at 10 °C/min. Microanalysis was carried out by using a 240XA Model CHN analyzer calibrated to NBS-SRM-141c acetanilide; the quality control standard was NBS-SRM-148 nicotinic acid. Elemental analyses of Si, Mg, and Li in the clays were determined as weight percent of the oxides. Measurements of SiO_2 and MgO were made according to ASTM standard test method 3682. Li_2O was determined by digestion of the sample in aqua regia and HF, followed with analysis by flame atomic absorption spectrophotometry. Reproducibility ranges for SiO_2, MgO, and Li_2O are 4 wt %, 0.2 wt %, and 0.02 wt %, respectively. For fluoride analysis, samples were pyrohydrolyzed at 900 °C and collected in a sodium carbonate–sodium bicarbonate solution; these solutions were then analyzed by ion chromatography.

Table I. X-ray Diffraction Results for Organic-Containing Crystallized Hectorites and Ion-Exchanged Hectorites[a]

synthetic clay	d(001), Å	ion-exchanged clay	d(001), Å
TMA–hectorite	14.3	TMA–SLH	14.3
TMPyP–hectorite	15.0	TMPyP–SLH	14.0
TAP–hectorite	16.7	TAP–SLH	15.0
FeTAP–hectorite	17.4	FeTAP–SLH	16.4

[a] Samples analyzed as oriented films. TMA = tetramethylammonium; TMPyP = tetrakis(*N*-methyl-4-pyridiniumyl)porphyrin; TAP = tetrakis(*N*,*N*,*N*-trimethyl-4-aniliniumyl)porphyrin; SLH = synthetic Li^+–hectorite.

Small-angle neutron-scattering (SANS) measurements were made on the small angle diffractometer (SAD) at the Intense Pulsed Neutron Source (IPNS) of Argonne National Laboratory. This instrument is based on a pulsed neutron source and uses a white beam and time-of-flight techniques. The neutrons employed have wavelengths in the range 0.5–14 Å, binned into 67 wavelength channels with a 5% wavelength spread in each channel. The flux of the incident neutrons is monitored with a BF_3 detector, and the scattered neutrons are detected by a 20 × 20 cm^2 ^3He area detector with 64 × 64 spatial channels. The q range covered is 0.005–0.35 $Å^{-1}$ in a single measurement. For further details of the instrument, data acquisition, and data reduction, the reader is referred elsewhere.[8] Solution samples of clay slurries in D_2O were contained in 2 mm path length Suprasil cells (Quaracell Products). Scattering is greatly enhanced by using D_2O in place of H_2O in the clay synthesis due to differences in the scattering length density of ^2D vs ^1H. The scattering measurements took 1–5 h depending upon the sample.

Analysis of SANS Data. The small-angle scattering of systems such as particles in a solution can be analyzed by using the Guinier approximation,[9] which is described by

$$I(q) = NV^2(\Delta\rho)^2 \exp(-q^2R_g^2/3)$$

In this equation, N is the number of particles, V is the volume of the particle, $(\Delta\rho)$ is the difference in the scattering length density of the particle and the solvent, R_g is the radius of gyration (root-mean-square distance of the atoms from the centroid of the scattering particle), and q is the wave vector $4\pi(\sin\theta)/\lambda$, where 2θ is the Bragg scattering angle and λ is the wavelength. A plot of ln $[I(q)]$ vs q^2 will yield a linear curve in the limit of $qR_g \leq 1$ with a slope proportional to R_g. In addition, the intensity at $q = 0$ is proportional to the number of scattering particles and the square of their molecular weight.

In the case of rodlike particles, the SANS data will yield a cross-sectional radius of gyration R_c. The modified Guinier law[10] for a rod can be expressed as

$$I(q) \propto (1/q) \exp[(-q^2R_c^2)/2]$$

R_c can be obtained from the slope of the straight line in a plot of ln $[q\,I(q)]$ vs q^2. The radius of the rod is determined from the relation $R = R_c\sqrt{2}$. For sheetlike particles that are extremely large in two dimensions but have a finite thickness, the SANS data give a thickness factor R_t. The modified Guinier law for sheet[9] can be expressed as

$$I(q) \propto 1/q^2 \exp(-q^2R_t^2)$$

(7) *Natl. Stand. Ref. Data Ser. (U.S., Natl. Bur. Stand.)* **1981**, *NSRDS-NBS 25*, Sect. 18.

(8) Epperson, J. E.; Thiyagarajan, P.; Klippert, T. E. SAD Manual. Available from IPNS, Argonne National Laboratory, Argonne, IL 60439.

(9) Guinier, A.; Fournet, G. *Small-Angle Scattering*; Walker, C. B., Yudowitch, K. L., Translators; Wiley: New York, 1955; p 19.

(10) Kratky, O.; Pilz, I. *Q. Rev. Biophys.* **1978**, *11*, 39.

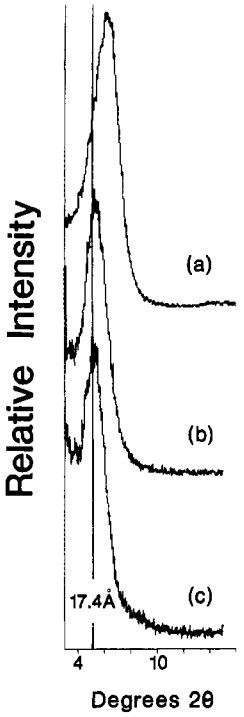

Figure 1. X-ray powder diffraction (001) reflections of (a) synthetic Li^+–hectorite (SLH), (b) iron(III) tetrakis(*N*,*N*,*N*-trimethyl-4-aniliniumyl)porphyrin–SLH (FeTAP–SLH), and (c) crystallized Fe^{III}TAP–hectorite.

R_t is obtained from the slope of the straight line in the $\ln[(q^2 I(q)]$ vs q^2 plot. The thickness of the lamella can be obtained by multiplying R_t by $\sqrt{12}$. The above approximation is based on the fact that the scattering intensity varies as $1/q^2$ for infinitely large sheets in two dimensions with an infinitesimal thickness. This correlation breaks down at finite minimum q values depending upon the distance correlations in the other two dimensions (surface area). If the surface area is larger, the q value at which the breakdown occurs will become smaller, and vice versa. The breakdown in the correlation typically shows up as a bendover in the low-q region of the modified Guinier plot for a sheet. A modified Guinier plot for a sheet thus yields the thickness of the sheet (from the slope of a straight line in the low-q region), as well as the qualitative extent of its surface area (from the q value at which the bendover occurs).

Results and Discussion

X-ray Diffraction. Figure 1 displays the X-ray diffraction (XRD) spectra of a series of hectorites: synthetic Li^+–hectorite (SLH), Fe^{III}TAP-exchanged SLH, and crystallized, synthetic Fe^{III}TAP–hectorite. Since these were analyzed as oriented thin films, the (001) reflections are preferred, while (*hk*0) reflections are not observed. Similar data obtained for other clay systems are summarized in Table I. XRD spectra of the samples run as powders contain typical smectite (*hk*0) peaks, e.g. 4.38 Å (020), 2.57 Å (130, 200), and 1.522 Å (060). The *d* spacing increases from 14.3 Å, when Li^+ ions are in the gallery (for SLH), to 16.4 Å, upon ion exchange with Fe^{III}TAP. The synthetic crystallized sample of FeTAP–hectorite displays a larger *d* spacing of 17.4 Å.

The *d* spacing of a clay includes the dimensions of the clay layer itself—for a typical smectite this is 9.6 Å.[1] The experimentally observed *d* spacing corresponds to the combination of this value with the calculated size of the exchangeable cation in the free interlayer space or gallery. In this case, the thickness of the porphyrin molecule is the relevant measurement. Stone and Fleischer[11] have demonstrated that, for the free-base form of a porphyrin, the substituents on the porphyrin nucleus are tilted significantly out of the plane with respect to the inner nitrogen-containing macrocycle. By contrast, the substituents of the dication form, where all four inner nitrogens are protonated, are nearly coplanar with the macrocycle, thus leading to a "flatter" molecule. The observed thickness of an intercalated clay layer is therefore expected to be larger when the free base is present. Molecular modeling of TAP gives dimensions of about 17 × 17 × 7.1 Å for the free base and 17 × 17 × 6.3 Å for the dication.[3] Values are similar for TMPyP, although the thickness is less due to less bulky substituents (for example, tetraphenylporphyrin is roughly 4.6 Å thick[12]). Synthetic TAP–hectorite has a *d*(001) = 16.7 Å, which corresponds to a gallery height of 7.1 Å; this is identical with that expected for the free-base form of TAP. The gallery height of synthetic Fe^{III}TAP–hectorite is larger (7.8 Å), which may be due to the presence of the fifth ligand on the Fe(III) ion; likely candidates are a water molecule or hydroxyl group.

Table I lists XRD data for porphyrin-containing clays including the TAP system described above in detail. The synthetic crystallized samples always exhibit a larger *d* spacing than the corresponding ion-exchanged materials (1.0–1.7 Å difference). This suggests that the larger, free-base forms of the macrocycles remain intact throughout the hydrothermal crystallization process, which in fact is expected because the pH is relatively high (pH 8–9) under these conditions. In contrast, the dication form dominates following an ion-exchange procedure. Protonation to the dication is common for porphyrin-exchanged clays due to the acidic nature of clay surfaces.[3,13]

Table II lists results of microanalysis data for several porphyrin-containing clays. Weight percentages of carbon and nitrogen were determined and then C:N ratios were calculated and compared to theoretical values. Overall, the C:N ratios agree very well with the expected results, which indicates that the porphyrin macrocycles have not degraded. This is especially important for the synthetic crystallized systems where the porphyrins were subjected to aqueous reflux conditions for 2 days in a basic (pH 8–9) solution. Also included for comparison are results from porphyrin ion exchange with another synthetic hectorite; this clay is prepared by a sintering reaction at 800 °C and is called Li^+–fluorohectorite (LFH).[14]

Elemental analysis results of synthetic, crystallized hectorite samples are summarized in Table III. Since excess Si and Li were present in all samples, compositions were calculated on the

Table II. Microanalysis Data for Porphyrin-Containing Clays

sample	% C	% N[a]	C:N exptl	C:N theor
TMPyP–hectorite	6.6	1.4	5.5	5.5
TMPyP–SLH	4.4	0.3[b]		5.5
TMPyP–LFH[3]	8.3	1.7	5.7	5.5
TAP–hectorite	7.4	1.2	7.2	7.0
TAP–SLH	6.6	1.1	7.0	7.0
TAP–LFH[3]	7.8	1.3	7.0	7.0

[a] Accuracy and precision is ±0.3 wt %. [b] Measurement at limit of detection, considered unreliable. TMPyP = tetrakis(*N*-methyl-4-pyridiniumyl)porphyrin; TAP = tetrakis(*N*,*N*,*N*-trimethyl-4-aniliniumyl)porphyrin; SLH = synthetic Li^+–hectorite; LFH = Li^+–fluorohectorite (data taken from ref 3).

Table III. Elemental Analysis of Synthetic, Crystallized Hectorite Clays[a]

	SLH	TAP–hectorite	TMPyP–hectorite
wt % SiO_2	60.6	61.8	62.5
wt % MgO	17.6	13.1	13.8
wt% Li_2O	2.11	1.21	1.13
wt % F	2.4	4.2	2.2
wt % C, H, N	...	9.28	8.47

[a] Estimated relative precisions are ±3% for SiO_2, ±5% for MgO, and ±4% for Li_2O. SLH = synthetic Li^+–hectorite; TMPyP = tetrakis-(*N*-methyl-4-pyridiniumyl)porphyrin; TAP = tetrakis(*N*,*N*,*N*-trimethyl-4-aniliniumyl)porphyrin.

(11) Stone, A.; Fleischer, E. B. *J. Am. Chem. Soc.* **1968**, *90*, 2735.
(12) Cady, S. S.; Pinnavaia, T. J. *Inorg. Chem.* **1978**, *17*, 1501.
(13) VanDamme, H.; Crespin, M.; Obrecht, F.; Cruz, M. I.; Fripiat, J. J. *J. Colloid Interface Sci.* **1978**, *66*, 43.
(14) Barrer, R. M.; Jones, D. L. *J. Chem. Soc. A* **1970**, 1531.

Table IV. Synthetic Hectorite Compositions: $Si_8(Mg_{5.34}Li_{0.66})O_{20}(OH,F)_4[Ex_{0.66/n}]^{n+}$ [a]

clay	$[Ex_{0.66/n}]^{n+}$	amt, mol F	amt, mol excess SiO_2	amt, mol excess Li
SLH	$Li_{0.66}$ (n = 1)	1.54	4.3	0.42
TAP-hectorite	$TAP_{0.18}$ (n = 4)	3.62	8.9	0.67
TMPyP-hectorite	$TMPyP_{0.19}$ (n = 4)	1.81	8.2	0.53

[a] SLH = synthetic Li^+-hectorite; TMPyP = tetrakis(N-methyl-4-pyridiniumyl)porphyrin; TAP = tetrakis(N,N,N-trimethyl-4-aniliniumyl)porphyrin.

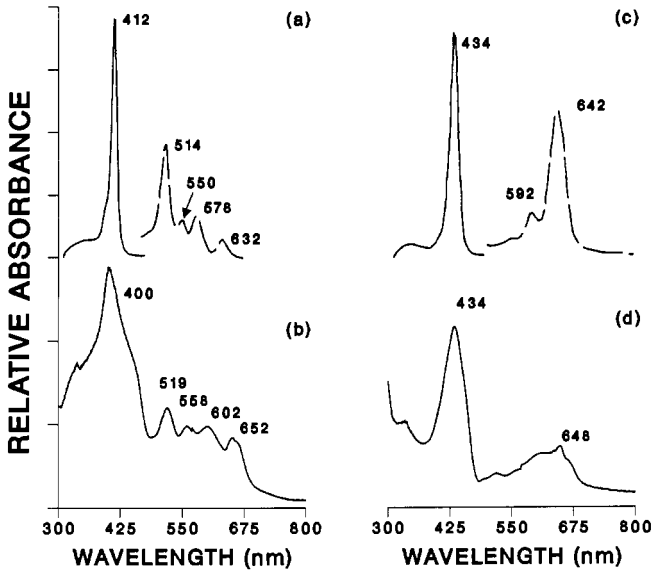

Figure 2. UV-visible absorption spectra of tetrakis(N,N,N-trimethyl-4-aniliniumyl)porphyrin (TAP): (a) TAP in distilled water; (b) synthetic TAP-hectorite, (c) TAP in 1 N HCl; (d) TAP-SLH. The top traces are solution spectra; dashed curves represent more concentrated solutions. The bottom traces are diffuse reflectance spectra.

basis of the ideal fluorohectorite formula: $Si_8(Mg_{5.34}Li_{0.66})O_{20}(OH,F)_4[Ex_{0.66/n}]^{n+}$. In fluorohectorites, a certain percentage of lattice hydroxyl groups are replaced by fluoride ions. For instance, the synthetic fluorohectorite termed laponite has been given the formula[15] $Si_8(Mg_{5.36}Li_{0.60})O_{20}(OH_{1.50}F_{2.50})Ex^+_{0.70}$. Table IV lists the identity and amount of the exchangeable cation (Ex) for each clay, the amount of fluoride analyzed, and the amounts of silica and lithium impurities. The absence of non-clay peaks in XRD spectra from 3 to 70° 2θ precludes the presence of crystalline impurities such as lithium oxides, lithium silicates, quartz, or unreacted LiF. Data from Table IV reveal that reasonable amounts of Ex are present in each clay, which again demonstrates the integrity of the crystallized samples. Layer-lattice charges of the synthetic clays are considered to be comparable to those of natural hectorites on the basis of these determined structural compositions.

UV-Visible Absorption Spectroscopy. UV-visible absorption spectroscopy is a powerful and commonly used diagnostic tool for the characterization of porphyrins. It can be used not only to examine the integrity of the macrocycles in their clay environment but also to observe subtle solvent effects and to determine free-base versus mono- and dication forms. Absorption bands in the UV-visible region occur in two sets for porphyrins. The Soret band is characterized by a large extinction coefficient and lies in the 400–450-nm range. A second set of weaker bands occurs between 450 and 700 nm; free bases have four bands in this region. Protonation to the dication causes the Soret band to shift to higher wavelength and decreases the number of weaker bands to 2. This behavior is highlighted in Figure 2 for TAP in water as the free base (H_2P) and in 1 N HCl as the dication (H_4P^{2+}).

Table V. UV-Visible Absorption Data for Tetrakis(N-methyl-4-pyridiniumyl)porphyrin in Solution and in Clays[a]

species	wavelength, nm
free base[b]	422, 518, 554, 584, 640
dication[b]	446, 591, 642
synthetic hectorite	441, 610
SLH	464, 490, 612
Ca-montmorillonite	423, 600
H^+-montmorillonite	438, 615
LFH	431, 609
HAW	423, 589

[a] SLH = synthetic Li^+-hectorite; LFH = Li^+-fluorohectorite; HAW = hectabrite AW, a natural hectorite. [b] Solution spectra; the others are DR spectra.

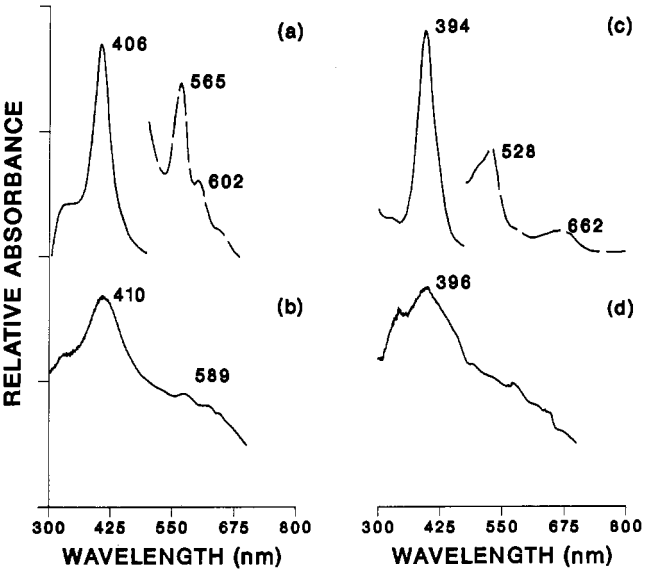

Figure 3. UV-visible absorption spectra of iron(III) tetrakis(N,N,N-trimethyl-4-aniliniumyl)porphyrin (FeTAP): (a) FeTAP in distilled water; (b) synthetic FeTAP-hectorite; (c) FeTAP in 1 N HCl; (d) FeTAP-SLH. The top traces are solution spectra; dashed curves represent more concentrated solutions. The bottom traces are diffuse reflectance spectra.

Figure 2 also contains diffuse reflectance (DR) absorption spectra of TAP-containing clays, both crystallized and ion-exchanged. These spectra are typical of porphyrin-exchanged clays.[3,15] The spectrum of crystallized TAP-hectorite contains characteristics of the free-base form of the porphyrin, which agrees with the X-ray diffraction results. The shifting of the Soret band to a lower wavelength (400 nm) is probably influenced by the clay environment and may be related to solvent effects.[16] Ion-exchanged TAP-SLH, on the other hand, displays a DR spectrum that can be correlated to the H_4TAP^{2+} dication. Again, this agrees with the XRD results, where the dication is indicated by a smaller d spacing. Corresponding UV-visible absorption solution and DR data for the TMPyP systems are summarized in Table V. However, as discussed elsewhere,[3] the DR spectra of TMPyP-clay systems do not readily lend themselves to diagnostic analysis in this respect. Shifts in the Soret band are strongly affected by the clay environment, and all fine structure in the wavelength range of the less intense bands is lost—these bands average out into one intense, broad peak spanning over 80 nm. Even the most acidic clay examined, H^+-exchanged montmorillonite, does not show appreciable differences from other clays, nor does it closely resemble the solution dication spectrum of TMPyP.

UV-visible absorption data for the metalloporphyrin FeTAP system are illustrated in Figure 3. The synthetic crystallized FeTAP-hectorite spectrum matches that of FeTAP dissolved in water very closely. The spectrum of ion-exchanged FeTAP-SLH,

(15) Neumann, B. S. *Rheol. Acta* **1965**, *4*, 250.

(16) Bergaya, F.; VanDamme, H. *Geochim. Cosmochim. Acta* **1982**, *46*, 349.

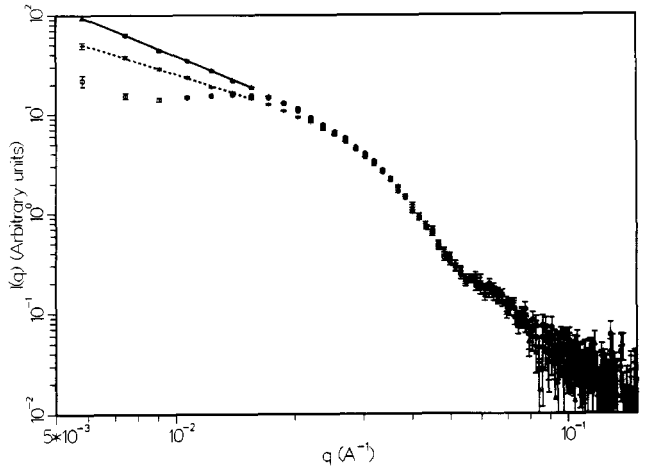

Figure 4. log I vs log q plot of the small-angle neutron scattering for the tetrakis(*N*-methyl-4-pyridiniumyl)porphyrin–silica sol system: (○) silica sol; (△) unheated TMPyP–silica sol with slope (—) of −1.64; (+) heated TMPyP–silica sol with slope (- - -) of −1.27.

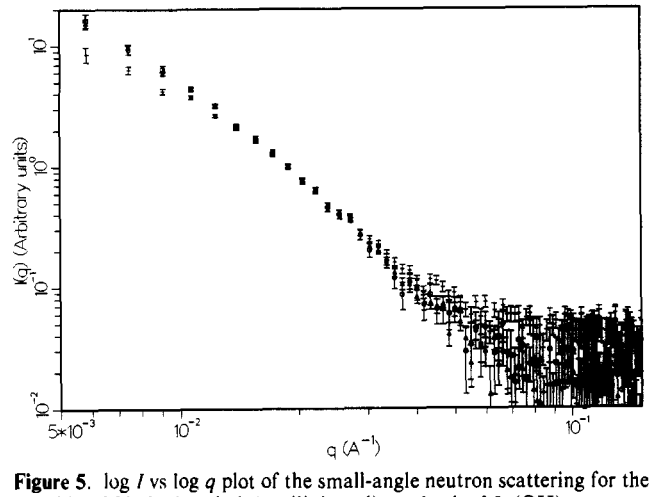

Figure 5. log I vs log q plot of the small-angle neutron scattering for the tetrakis(*N*,*N*,*N*-trimethyl-4-aniliniumyl)porphyrin–$Mg(OH)_2$ system: (○) $Mg(OH)_2$; (△) unheated TAP–$Mg(OH)_2$; (+) heated TAP–$Mg(OH)_2$.

however, more closely agrees with that of FeTAP dissolved in 1 N HCl, again demonstrating the more acidic nature of this system. The differences between water and dilute acid for FeTAP are explained by the known sensitivity of UV–visible absorption behavior to the associated anion of +3 cations.[17]

Small-Angle Neutron Scattering. Porphyrin interactions with each of the major gel constituents were first examined separately, and then the porphyrin–clay synthetic gel system was probed.

TMPyP–Silica System. SANS data for the TMPyP–silica system are expressed as a log I vs. log q plot in Figure 4. Ludox HS-30 (30% silica in solution) was diluted in D_2O to 16.7% by weight, which gives a silica sol concentration of about 5%. Although the average particle size is quite small (120 Å as quoted by the supplier), Guinier analysis cannot be carried out due to the presence of strong interparticle interactions. The peak position (q = 0.014 Å^{-1}) is equivalent to a particle–particle distance of 448 Å.

Upon addition of porphyrin (in this case TMPyP), the interaction between negatively charged silica particles is highly perturbed by the cationic macrocycles. The log–log slope in the low-q region of the plots (Figure 4) is −1.64 for an unheated sample and −1.27 for a sample refluxed for 2 days. Scatterings in the q region of 0.02–0.25 Å^{-1} are nearly identical for all three samples. Therefore, it appears that the colloidal silica particles remain intact upon addition of porphyrin, even after refluxing; it is also possible that unreacted silica exists. A modified Guinier analysis for a

(17) Abdo, S.; Cruz, M. I.; Fripiat, J. J. *Clays Clay Miner.* **1980**, *28*, 125.

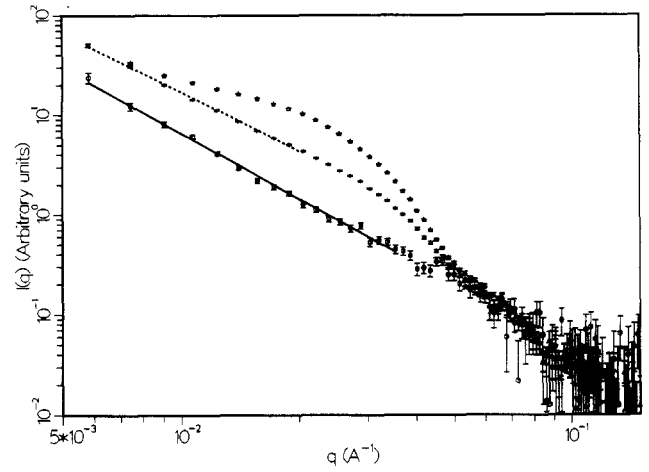

Figure 6. log I vs log q plot of the small-angle neutron scattering for the synthetic tetrakis(*N*-methyl-4-pyridiniumyl)porphyrin–hectorite synthesis system: (○) natural hectorite with slope (—) of −2.18; (△) unheated TMPyP–hectorite gel; (+) heated TMPyP–hectorite gel with slope (- - -) of −2.0.

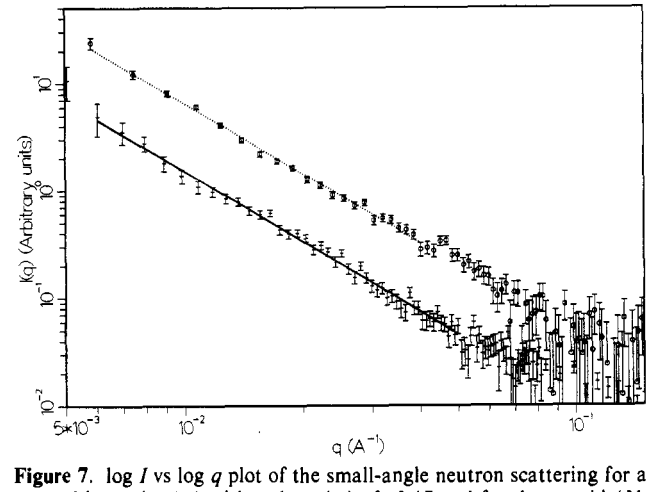

Figure 7. log I vs log q plot of the small-angle neutron scattering for a natural hectorite (○) with a slope (···) of −2.17 and for the tetrakis(*N*-methyl-4-pyridiniumyl)porphyrin-exchanged natural hectorite (+) with a slope (—) of −2.18.

rod (ln [q $I(q)$] vs q^2) was performed, but no linear regions were found; this suggests that the sol and the porphyrin have interacted to form a random network.

Porphyrin–$Mg(OH)_2$ System. Log I vs log q plots for colloidal $Mg(OH)_2$ and the mixture of TAP–$Mg(OH)_2$ (both before and after heating) are shown in Figure 5. Guinier analysis of the data (ln I vs q^2) does not yield a linear region for $Mg(OH)_2$, indicating either that the particle size is quite large (in a Guinier region inaccessible for the instrument) or that the system is polydisperse in nature. The addition of TAP does not alter the scattering data appreciably. The $Mg(OH)_2$ scattering is so dominant that any subtle differences between porphyrins, although none are expected, were not noticeable. Upon heating, the particle size of this system decreases, as seen by the slower variation of $I(q)$ as a function of q in the low-q region. Thus, addition of porphyrin is seen to have little effect on $Mg(OH)_2$ particles. This is consistent with XRD data, which display strong reflections indicative of brucite (a natural layered magnesium hydroxide) that only decrease slightly in intensity after heating.

TMPyP–Hectorite Gel System. The log I vs log q plots for the TMPyP–hectorite gel system are shown in Figure 6, along with a natural hectorite control sample. Scattering for the hectorite control mineral clearly indicates a lamellar structure (slope = −2.18 in the low-q region). A porphyrin-exchanged natural hectorite was also examined and compared in Figure 7 to the natural hectorite, and the scattering curves are nearly identical in slope. For the unheated TMPyP–hectorite gel, a hump in the middle-q

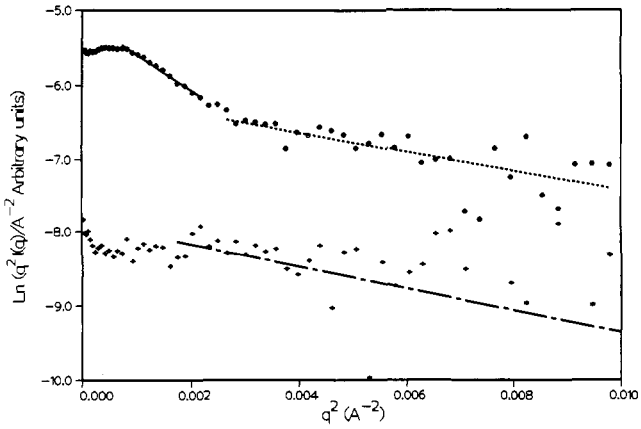

Figure 8. Modified Guinier sheet analysis of the synthetic tetrakis(*N*-methyl-4-pyridiniumyl)porphyrin–hectorite heated gel (O), which displays two different slopes corresponding to thicknesses of (—) 85 ± 8 Å and (- - -) 43 ± 14 Å. The analysis is also done for the natural hectorite control mineral (+), which has a slope (– – –) corresponding to a thickness of 38 ± 20 Å.

region (0.01–0.05 $Å^{-1}$) indicates the presence of a high degree of aggregation. The log–log slope of the heated sample increases to −2.0, suggesting that the compound is forming a layered structure. In addition, heating causes a decrease in the scattering of the middle-q region. The generally accepted mechanism of formation of hectorite involves the condensation of tetrahedral silica layers on preexisting brucitic sheets. The destruction of the random network structure characteristic of the porphyrin–silica system in the presence of the brucitic sheets may be responsible for the disappearance of this hump. The high-q regions for both the TMPyP–hectorite and the hectorite control are quite similar. These characteristics combine to suggest that heating a TMPyP–hectorite gel causes the initial large aggregates to break down and lead to the formation of inorganic layers with porphyrin macrocycles between them. Longer reaction times of porphyrin–clay crystallizations result in delamination of the clay layers. The short-range ordering of the clay along the c axis is clearly evident in SANS spectra of gels heated for up to 5 days, with log–log slopes of −2.2. No d spacing is observed in XRD spectra, although other clay peaks are readily seen.

Figure 8 displays modified Guinier plots [ln (Iq^2) vs q^2] for the hectorite control sample in D_2O and for the heated synthetic TMPyP–hectorite gel system. Analysis of these data yields a thickness of 38 ± 20 Å for the hectorite control and thicknesses of 43 ± 14 and 85 ± 8 Å, and a bendover in the very low q region for the heated TMPyP–hectorite system. The bendover indicates that the lamella have finite surface areas. Thus, the SANS data for the synthetic TMPyP–hectorite system clearly show that intercalated lamellar structures exist with large thicknesses and finite surface areas.

Conclusions

The Barrer synthesis[6] of alkylammonium hectorites typically requires from 5 to 7 days for completion. The present process, which incorporates water-soluble porphyrins as the organic phase, needs only 2 days for formation of a clay mineral. This is a significant decrease in reaction time that may possibly be due to a "templating" action of the large, flat organic macrocycle. Charge distribution and size and shape of a templating molecule are believed to cause structure-directing behavior.[4] On the other hand, alteration of gel chemistry by an additive may be of equal or greater importance than the templating action.[4] When one template can be used to direct several different frameworks, structural control is exercised by other synthesis variables such as temperature, time, template concentration, gel oxide composition, and pH.[5] Although Si:Al ratios, concentrations, and temperatures have all been held constant, the effects of other factors in the gel chemistry, such as pH, have not been entirely ruled out. Slight modifications in the ionic nature of the gel could shift the composition of the nucleated gel to a more favorable composition for crystallization. Therefore, a strict interpretation of the template effect cannot as yet be applied with certainty.

The use of porphyrins also offers many advantages in terms of synthetic strategies and final applications. Substituents on the porphyrin, in this case the alkylammonium units, can be easily derivatized. Porphyrins are in general well-known for both their biological and catalytic activity,[18] and potential uses can be based on these properties. X-ray absorption studies of iron(III) and copper(II) metalloporphyrin-containing synthetic clays are currently in progress to elucidate the local coordination environment of the transition-metal ion in detail.

Finally, SANS was employed as a powerful tool for probing interactions at the particulate level in the gel. Crystallization mechanisms and organic–inorganic interactions in systems such as these are in general not well understood. Porphyrin reacted with a silica sol alone was demonstrated to lead to a random network structure. Porphyrin reacted with magnesium hydroxide alone did not alter the precipitation of the layered mineral brucite $Mg(OH)_2$. However, when porphyrin, silica, and $Mg(OH)_2$ were reacted together in the clay synthesis gel (which also contains LiF), the layered clay phase was observed. Experiments utilizing the unique ability of SANS to probe organic–inorganic interactions by contrast-variation techniques are planned in order to resolve the issue of templating vs alteration of gel chemistry for porphyrins in clay syntheses.

Acknowledgment. This work has benefited from the use of the Intense Pulsed Neutron Source at Argonne National Laboratory. The D_2O used for SANS experiments and hectabrite AW were graciously provided by H. Crespi of ANL and Dr. I. E. Odom of American Colloid Co., respectively. Ludox HS-30 silica sol was donated by Du Pont. The technical assistance of A. G. Stellpflug is acknowledged. The Analytical Chemistry Division of ANL performed microanalysis and elemental analysis determinations. This work was performed under the auspices of the Office of Basic Energy Sciences, Division of Chemical Sciences, U.S. Department of Energy, under Contract No. W-31-109-ENG-38.

(18) Dorough, G. D.; Miller, J. C.; Huennekens, F. M. *J. Am. Chem. Soc.* **1951**, *73*, 4315.
(19) Smith, K. M. *Porphyrins and Metalloporphyrins*; Elsevier Scientific: Amsterdam, 1975.